Partitioning, Fractionation, and Conformations of Star Poly(ethylene glycol) in Isobutyric Acid and Water

Alexander I. Norman,*,†,‡,§ Derek L. Ho,|| and Sandra C. Greer*,†,‡

Department of Chemical and Biomolecular Engineering and Department of Chemistry and Biochemistry, The University of Maryland College Park, College Park, Maryland, 20742, and The Electronic Materials Group, Polymers Division, National Institute of Standards and Technology, Gaithersburg, Maryland, 20899

Received July 13, 2007; Revised Manuscript Received October 16, 2007

ABSTRACT: We investigate the partitioning, fractionation, and conformations of star poly(ethylene glycol) (PEG) in coexisting liquid phases of isobutyric acid and water. Star PEG does partition: 98% in the upper isobutyric acid phase, versus 80−90% for linear PEG. There is no significant fractionation of the star PEG for molecular masses less than or equal to 10 kg/mol, but fractionation may occur at higher molecular masses. Small angle neutron scattering shows that the arms of the star PEG molecules form coils in D_2O but form stiff rods in deuterated isobutyric acid. At higher average molecular masses (>4 kg/mol) and higher temperatures (60 °C), some arms are coils and some are rods in isobutyric acid. Polarimetry studies indicate that these "rodlike" arms are actually helical conformations. At a star molecular mass of 2 kg/mol, the helical arms persist above 70 °C, but at larger molecular masses, the helical arms revert to coils at temperatures around 75 °C. The addition of PEG to isobutyric acid and H_2O increases the critical temperature of the solvent mixture, and the increase is less as the star branching increases.

Introduction

The architecture of a polymer, linear, star, randomly branched, etc., greatly influences its properties, both in the bulk and in solution.[1−4] A star polymer has a single, central branch point from which emanate several linear polymer chains or "arms" of about the same chain length. Linear polymers coil into random, fluctuating shapes in good solvents, but star polymers are "more packed and spherical than linear ones having the same molecular weight"[5] and have been termed "ultrasoft colloids."[6] Star polymers have many industrial and biological applications, including uses as melt-strengtheners,[7] coatings,[8] and "enhancers of antibody−antigen reactions."[9]

We have previously reported the dramatic partitioning and fractionation of linear poly(ethylene glycol) (PEG) in a two-phase mixture of isobutyric acid and water.[10,11] Most of the PEG partitions into the upper, isobutyric acid-rich phase, even though PEG is much more soluble in water than in isobutyric acid. When the molecular mass is greater than about 10 kg/mol, the polymer fractionates quite dramatically between the two phases: PEG chains of lower average molecular mass migrate to the upper isobutyric acid-rich phase, and chains of higher average molecular mass predominate in the lower water-rich phase. The partitioning and fractionation are related to the difference in the conformation of linear PEG in each solvent: linear PEG molecules form coils in water but form helices in isobutyric acid.[12−14]

Now we explore the effects of the architecture of the PEG molecules on the partitioning, fractionation, and conformations in isobutyric acid and water. We address the following questions.

(1) How does the addition of star PEG affect the upper critical solution temperature (UCST) for isobutyric acid and water? When "impurities" are added to a binary liquid mixture with an UCST, then the UCST is shifted.[15] If the impurity is a polymer, then the change in the UCST can depend on both the concentration and the molecular mass of the polymer, while the critical volume fraction is not very sensitive to low levels of the polymer.[16−23] The UCST of isobutyric acid and water *increases* upon addition of linear PEG.[11,13] PEG is more soluble in water than in isobutyric acid, which makes the two solvents mutually less soluble and thus raises the UCST. Now we learn that four-arm star and six-arm star PEG also increase the UCST of isobutyric acid and water. The effect on the UCST decreases as the chain branching increases, but the dependence on molecular mass is about the same for star PEG as for linear PEG.

(2) Are the partitioning and fractionation of star PEG in isobutyric acid and water different from the partitioning and fractionation of linear PEG in this solvent mixture? When there is a difference in the interaction of a polymer unimer with each of the two coexisting liquid phases, then that interaction is amplified as the polymer chain gets longer and longer, and there is more fractionation for larger polymers, as is indicated by mean field theories of fractionation.[24] Fractionation is important as a method of polymer purification.

Case studied PEG fractionation between the mutually insoluble liquids water and hexane.[25,26] Rintzler Yen and coworkers[27] studied the fractionation of star PEG near the lower critical solution temperature (LCST) of PEG in aqueous salt solutions and had some success in fractionating the star PEG molecules and reducing the polydispersity by a multistep process. Linear PEG fractionates between liquid and gas phases in supercritical CO_2 or CH_3CClF_3,[28,29] and the latter can even separate star and linear PEG.[28]

We have previously studied the partitioning and fractionation of linear PEG in isobutyric acid and water.[10,11] We found high degrees of partitioning and fractionation that increase with

* To whom correspondence should be addressed. E-mail: alex.norman@nyu.edu (A.I.N); sgreer@umd.edu (S.C.G).
† Department of Chemical and Biomolecular Engineering.
‡ Department of Chemistry and Biochemistry.
§ Current address: Molecular Design Institute, Department of Chemistry, New York University, 100 Washington Square East, New York, New York 10003.
|| National Institute of Standards and Technology.

10.1021/ma071568w CCC: $37.00
Published on Web 11/28/2007

Table 1. Molecular Weights of the Total Chain of the Star PEG Samples and Their Corresponding UCST in Mixtures of IBA and H_2O

polymer	studies[a]	lot no.[b]	$10^3 \times M_w$ (g/mol)	$10^3 \times M_n$ (g/mol)	M_w/M_n	T_c[c] (°C)
4-arm star 2k	F, S, P	P2153-4EOOH	2.2	1.8	1.3	28.6
6-arm star 4k	F, S, P	P2800-6EOOH	2.8	2.5	1.1	28.5
4-arm star 10k[d]	F, S, P	P1672-4EOOH	11.7	8.8	1.3	40.9
6-arm star 10k	F, S, P	P2833-6EOOH	17.8	16.3	1.1	45.8
4-arm star 20k[d]	F, P	P1626-4EOOH	27.6	23.2	1.2	59.8
6-arm star 20k[d]	F, P	P1855-6EOOH	36.3	31.5	1.2	65.0

[a] F, fractionation studies done; S, SANS studies done, P, polarimetry studies done. [b] All samples from Polymer Source (Quebec). [c] Polymer concentration = 2.20 ± 0.01 mg/mL. [d] Low molecular mass impurities present.

increasing molecular mass of the linear PEG; partitioning occurs at all polymer molecular masses, fractionation occurs only at molecular masses above about 10 kg/mol. We show below that star PEG also partitions between the phases of isobutyric acid and water, even more than does linear PEG of the same molecular mass. We did not observe fractionation of the star PEG at molecular masses less than or equal to 10 kg/mol, but fractionation may occur at higher molecular masses.

(3) What are the conformations of star PEG in water and in isobutyric acid? We have shown that linear PEG molecules form coils in water and form helices in isobutyric acid and that the helices in isobutyric acid revert to coils at higher temperatures.[12−14] We then expect that star PEG molecules in water will have flexible arms, but that star PEG molecules in isobutyric acid will have rigid, helical arms. We show, using small-angle neutron scattering and polarimetry, that this is true and that the helix-to-coil transition for star PEG molecules occurs at higher temperatures for star PEG than for linear PEG molecules of the same molecular mass.

Experimental Methods

Materials. Commercial star PEG samples were used as received and are listed in Table 1. The number average and weight average molecular masses, M_n and M_w, and the polydispersities (M_w/M_n) were determined in our laboratory by size exclusion chromatography (SEC) (see below). The synthesis of star PEG can result in the presence of low molecular mass oligomers, of star polymers with different numbers of arms, and of star polymers with different arm lengths.[9] Impurities were observed in the SEC traces for 4-arm 10k, 4-arm 20k, and 6-arm 20k samples, appearing as peaks at low molecular mass and of low intensity. The molecular masses and distributions in Tables 1 and 2 were all determined from the SEC peaks of the star polymers, excluding the impurity peaks.

Three samples of linear PEG were used to determine the effect of linear PEG on the UCST, to compare to the effect of the star PEG. The linear PEG samples were samples 2kOH, 10kOH, and 20kOH that are described in our earlier paper.[12]

The solvents used were hydrogenated isobutyric acid (Aldrich, 99% purity), deuterated isobutyric acid (Isotech, 98% D), D_2O (Aldrich, 99.9% D), and freshly distilled deionized water (Nanopure system: Barnstead, 18.2 MΩ cm). The chiral dopant used in the polarimetry experiments was (*S*)-(+)- 1,2 propanediol (Lancaster Chemicals, 98% pure enantiomer).

Determination of the UCST for Star PEG in Isobutyric Acid and Water. Seven vials of solvent solution at the critical composition were prepared (2.50 g of H_2O + 1.60 g of isobutyric acid).[30] The star PEG samples listed in Table 1 were each added to a vial to a concentration of 2.20 ± 0.01 mg/mL. One sample was left as the solvent mixture without polymer. The vials were placed in a temperature-controlled water bath, heated above the UCST, and held at that temperature for several hours. The temperature was measured and controlled to within a few mK.[31] The temperature was then reduced in steps until critical opalescence occurred and phase separation followed.

Fractionation of Star PEG in Isobutyric Acid and Water. The procedure was the same as reported in our earlier work.[10,11] A critical composition[30] of 39 wt % isobutyric acid in H_2O and a polymer concentration of 2.20 ± 0.01 mg/mL were used throughout. Syringes were used to withdraw 1.0 mL samples from each coexisting liquid phase. The degree of partitioning of the star PEG chains was calculated from the ratio of the areas under the molecular mass distribution (MMD) of each phase.[11]

Size Exclusion Chromatography (SEC). Extracted samples were dried overnight in a vacuum oven, then rehydrated with 1.0 mL of water, and allowed to solvate for at least 12 h prior to SEC analysis. The M_n and M_w and polymer compositions were measured using a Waters SEC, as described elsewhere.[12]

Small-Angle Neutron Scattering (SANS). SANS experiments were carried out on the NG3 30 m SANS beamline at the NIST Center for Neutron Research (NCNR), Gaithersburg, Maryland. The details have been previously reported.[12,14]

Four star PEG samples (see Table 1) were investigated in pure D_2O and in pure deuterated isobutyric acid at concentrations of 12 ± 1 mg/mL. Samples were loaded into 1 mm path-length quartz cells and placed into a 10-position heating/cooling block. SANS data were recorded at 30 °C and 60 °C. Two sample-to-detector distances were used (13.24 and 1.38 m) to achieve a q range of 0.0034−0.4742 Å^{-1}. The neutron wavelength (λ) was 6 Å, with a wavelength spread ($\Delta\lambda/\lambda$) of 0.15. The 2D raw data were reduced to the intensity $I(q)$ vs q, where $q = (4\pi/\lambda)\sin(\theta/2)$, λ is the neutron wavelength and θ is the scattering angle, with incoherent background subtracted and corrections applied for background scattering from the cell and for detector nonlinearity, as described previously.[12,14]

SANS Data Analysis. The SANS data were analyzed using three different methods:[12,14,32] (1) scaling of the scattered intensity, $I(q)$, over a specific range of q; (2) modeling of the data using specific models for the shapes and interactions of the scattering particles; and (3) making the inverse Fourier transform of $I(q)$ into real space.

For the scaling analysis of $I(q)$ versus q, there are three regimes of interest: (1) the low q "Guinier" regime;[33] (2) the intermediate q regime (the fractal regime);[34] and (3) the high q "Porod" regime.[35] At low q, a plot of $\ln[I(q)]$ vs q^2 (the Guinier plot) allows the calculation of the radius of gyration, R_g. In the intermediate regime, $I(q)$ scales as $q^{-1/\upsilon}$, where υ is the Flory exponent.[24] Under θ conditions, a polymer chain will have an ideal random walk (Gaussian) with $\upsilon = {}^1/_2$, and $I(q)$ will scale as q^{-2}. In good solvents, (e.g., PEG in water), a polymer chain will have a self-avoiding (excluded volume) random walk with $\upsilon = {}^3/_5$, and $I(q)$ will scale as $q^{-5/3}$. For a stiff rod, $I(q)$ will scale as q^{-1}. In the high q regime, $I(q)$ scales as q^{-4} when there is a sharp interface between the scattering particle and the surrounding solvent.

A common way of displaying SANS data from star polymers is the Kratky plot,[36] where $I(q)$ is multiplied by a power of the wave vector, $q^{1/\upsilon}$. Thus $I(q)q^2$ is plotted against q for Gaussian chains, and $I(q)q^{5/3}$ is plotted against q for chains with excluded volume.[37] The Kratky plot for a star polymer has a peak that indicates the radius of gyration of one arm of the star; there is no peak in the Kratky plot for a linear polymer.[37,38] The intensity of the peak for a star polymer increases with an increasing number of arms in the star. It has been argued that this determination of the radius of gyration of the star arm is valid only for Gaussian chains,[37] but

Table 2. Values of Weight and Number-Average Molecular Masses (M_w and M_n) and Polydispersity (M_w/M_n) for the Parent and Daughter Phases of Each Polymer System

PEG sample	day	parent phase[a]	lower phase[a]	upper phase[a]
4-arm star 2k	1	$M_w = 2300$ $M_n = 1930$ $M_w/M_n = 1.2$	$M_w = 2270$ $M_n = 2020$ $M_w/M_n = 1.2$	$M_w = 2260$ $M_n = 1800$ $M_w/M_n = 1.3$
	3		$M_w = 2270$ $M_n = 2100$ $M_w/M_n = 1.1$	$M_w = 1910$ $M_n = 1650$ $M_w/M_n = 1.2$
	12		$M_w = 2220$ $M_n = 1960$ $M_w/M_n = 1.1$	$M_w = 2200$ $M_n = 1530$ $M_w/M_n = 1.4$
	15		$M_w = 2830$ $M_n = 2590$ $M_w/M_n = 1.1$ $w_{lower} = 2 \pm 1$ %	$M_w = 2670$ $M_n = 1420$ $M_w/M_n = 1.9$ $w_{upper} = 98 \pm 1$ %
	22	$M_w = 2620$ $M_n = 2240$ $M_w/M_n = 1.2$		
6-arm star 4k	1	$M_w = 3100$ $M_n = 2780$ $M_w/M_n = 1.1$	$M_w = 2880$ $M_n = 2580$ $M_w/M_n = 1.1$	$M_w = 3090$ $M_n = 2780$ $M_w/M_n = 1.1$
	3		$M_w = 2880$ $M_n = 2580$ $M_w/M_n = 1.1$	$M_w = 2970$ $M_n = 2560$ $M_w/M_n = 1.2$
	5		$M_w = 2980$ $M_n = 2670$ $M_w/M_n = 1.1$	$M_w = 3060$ $M_n = 2700$ $M_w/M_n = 1.1$
	12		$M_w = 2960$ $M_n = 2730$ $M_w/M_n = 1.1$ $w_{lower} = 3 \pm 3$ %	$M_w = 3160$ $M_n = 3100$ $M_w/M_n = 1.0$ $w_{upper} = 97 \pm 3$ %
	22	$M_w = 3700$ $M_n = 3340$ $M_w/M_n = 1.1$		
4-arm star 10k[b]	1	$M_w = 10\,500$ $M_n = 5300$ $M_w/M_n = 2.0$		
	4		$M_w = 17\,300$ $M_n = 13\,600$ $M_w/M_n = 1.3$	$M_w = 7400$ $M_n = 2600$ $M_w/M_n = 2.8$
	6		$M_w = 23\,200$ $M_n = 18\,000$ $M_w/M_n = 1.3$	$M_w = 6900$ $M_n = 2800$ $M_w/M_n = 2.5$
	28		$M_w = 24\,700$ $M_n = 12\,700$ $M_w/M_n = 1.9$ $w_{lower} = 1.7 \pm 0.5$ %	$M_w = 8400$ $M_n = 3800$ $M_w/M_n = 2.2$ $w_{upper} = 97.3 \pm 0.5$ %
	33	$M_w = 8100$ $M_n = 3800$ $M_w/M_n = 2.1$		
6-arm star 10k	1	$M_w = 18\,000$ $M_n = 16\,100$ $M_w/M_n = 1.1$	$M_w = 18\,700$ $M_n = 18\,\,700$ $M_w/M_n = 1.1$	$M_w = 17\,900$ $M_n = 16\,600$ $M_w/M_n = 1.1$
	3		$M_w = 19\,900$ $M_n = 19\,400$ $M_w/M_n = 1.0$	$M_w = 14\,800$ $M_n = 13\,700$ $M_w/M_n = 1.1$
	5		$M_w = 17\,100$ $M_n = 16\,300$ $M_w/M_n = 1.1$	$M_w = 15\,900$ $M_n = 14\,800$ $M_w/M_n = 1.1$
	12		$M_w = 19\,200$ $M_n = 18\,700$ $M_w/M_n = 1.0$	$M_w = 17\,300$ $M_n = 14\,900$ $M_w/M_n = 1.2$
	15		$M_w = 20\,000$ $M_n = 18\,500$ $M_w/M_n = 1.1$ $w_{lower} = 1 \pm 1$ %	$M_w = 20\,000$ $M_n = 17\,000$ $M_w/M_n = 1.2$ $w_{upper} = 99 \pm 1$ %
	22	$M_w = 20\,700$ $M_n = 17\,000$ $M_w/M_n = 1.2$		

[a] Error bars for the average molecular masses are about 10% of the mass value. [b] Low molecular mass impurities present.

many use the Kratky plot,[39,40] and it is at least a useful way of viewing the data.

Our previous work on SANS from linear PEG in D_2O used the two models (macros on the NCNR website) that fitted best to SANS data for linear PEG and for linear PEG in deuterated isobutyric acid:[12,14] a semiflexible chain with excluded volume[41] and a rigid rod,[33] respectively. Here, we consider the SANS from star polymers using the following models.

The simplest case of polymer chains is that of flexible, but not self-avoiding polymers, that obey Gaussian statistics and are described by the Debye function:[42]

$$I(q) = I(0)\left[\frac{2\{\exp(-u) + u - 1\}}{u^2}\right] \quad (1)$$

$$I(0) = NV^2(\Delta\rho)^2 \quad (2)$$

$$u = \langle R_g^2\rangle q^2 \quad (3)$$

$$\langle R_g^2\rangle = \frac{(Lb)}{6} \quad (4)$$

where N is the number of scattering particles, V is the scattering volume, $\Delta\rho$ is the contrast term (difference in scattering length density between particle and solvent), $\langle R_g^2\rangle$ is the ensemble average radius of gyration squared (of the whole polymer molecule), L is the contour length, and b is the statistical segment (Kuhn) length. Linear PEG forms coils in D_2O,[12,14] and each arm of a star PEG is likely to form such a coil in D_2O. On the length scale probed by SANS, the coiled linear polymer and the star polymer may be indistinguishable. We use this Debye function for a polymer coil to model the SANS data for star PEG in D_2O.

Benoit proposed an analytical expression for $I(q)$ for Gaussian star polymers where there are no correlations among star arms and no correlations among star polymers (i.e., the structure factor $S(q) \rightarrow 1$):[43]

$$I(q) = \frac{2}{\alpha^2}\left[\frac{\alpha}{f} - \frac{1}{f}\{1 - e^{-\alpha}\} + \frac{(f-1)}{2f}\{1 - e^{-\alpha}\}^2\right] \quad (5)$$

$$\alpha = \frac{f}{(3f-2)}[q^2(R_g^{star})^2] \quad (6)$$

where f is the number of arms of the star polymer and R_g^{star} is the radius of gyration of the star polymer. For polymers in a good solvent (e.g., PEG in water), the R_g^{star} of the entire star polymer is related[44] to the R_g^{arm}:

$$R_g^{star} = R_g^{arm}\left[\frac{3f-2}{f}\right]^{1/2} \quad (7)$$

We will also fit the Benoit expression to the SANS data for star PEG in D_2O.

Dozier, Huang, and Fetters proposed a model that takes into account the mass−mass correlations within the star polymer.[37] This model assumes the Daoud and Cotton blob model for a star polymer,[44] in which the inner part of the star is regarded as a succession of concentric rings of "blobs" of size ξ. Within each blob, the polymer chain is described as a self-avoiding random walk with excluded volume, i.e., a coil. Equation 8 shows that $I(q)$ of a star polymer is governed by two different length scales: the radius of gyration of the star polymer (R_g^{star}) and an internal correlation length (ξ) of the star (described below):

$$I(q) = I(0)\exp\left[\frac{-q^2R_g^{star}2}{3}\right] + \frac{4\pi\alpha}{q\xi}\left[\frac{\sin\{\mu\tan^{-1}(q\xi)\}}{\{1+q^2\xi^2\}^{\mu/2}}\right]\Gamma(\mu) \quad (8)$$

where $I(0)$ is the scattered intensity at $q = 0$, α is a fitting constant, $\mu = 1/(\upsilon - 1)$, and υ is the Flory exponent. $\Gamma(\mu)$ is the Gamma function, $\Gamma(\mu) = \int_0^\infty e^{-y}\, y^{\mu-1}\, dy$. This model was used by Willner et al.[39] to analyze the conformations of star poly(isoprene), star poly(butadiene), and star poly(styrene) in good solvents. We fit this model to the SANS data for star PEG in D_2O, but it is not suitable for star polymers that have arm conformations other than coils (such as helices).

The models above were fitted to the data using GraphPad Prism for Windows (version 4.03). The data points at very low q were not used because of the increase in $I(q)$ at very low q due to aggregation effects that cannot be included in the models.[45,46]

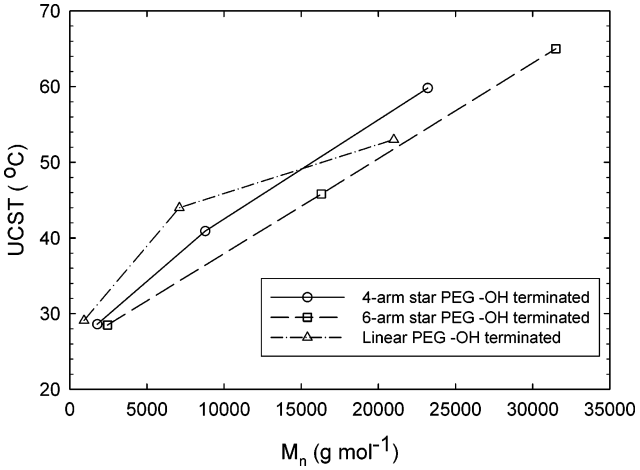

Figure 1. Variation of the UCST with molecular mass for linear, 4-arm star, and 6-arm star PEG in isobutyric acid and water at 2.20 ± 0.01 mg/mL. The error bars are smaller than the symbols and have not been shown.

The SANS data were also analyzed using the model free analysis GIFT (generalized indirect Fourier transformation) to yield the pair distance distribution functions, $p(r)$.[47−49] GIFT gives the average size and shape of the scattering particles and can be used for any polymer conformation. On the length scale probed by SANS, polymer molecules that form coils will have the $p(r)$ of spherical (or nearly spherical) entities, whereas polymer helices will have the $p(r)$ of rigid rods.

Polarimetry. Since PEG does not absorb in the UV, the usual detection of helices by circular dichroism is not feasible. Instead, we use polarimetry to detect the helical conformation of star PEG in isobutyric acid.[12,14] The PEG helices are equally likely to be left-handed and right-handed, so there is no net polarimetry signal from a solution of PEG helices. However, we found that if we introduce a chiral dopant at higher temperatures where the helices have reverted to coils, then the dopant biases the formation of the helices when the sample is cooled below the coil-to-helix transition temperature, and then the PEG helices do have a net optical rotation that can be used to track the folding and unfolding of the helices. The experimental procedure is the same as reported previously.[12,14]

Results and Discussion

1. The Effect of Star PEG on the UCST of Isobutyric Acid and Water. The values of the UCST for linear and star PEG samples at three molecular masses, all at a polymer concentration of 2.20 ± 0.01 mg/mL, are given in Table 1 and plotted in Figure 1. The addition of either linear PEG[11,13] or star PEG to isobutyric acid and water at the critical composition increases the UCST, and the increase is greater as the molecular mass increases. The UCST increases because PEG (linear or star) is more soluble in water than in isobutyric acid, thus makes the solvents less soluble in one another and increases the UCST, in accord with the Timmermans rules.[50] On the other hand, the effect of the PEG on the UCST decreases as polymer branching increases. This could be because the increased branching reduces the contact between the PEG molecules and the solvent.

We observed that the liquid−liquid meniscus remained in the center of the sample for all samples studied, indicating that the additions of star and linear PEG at this concentration have little effect on the critical composition of isobutyric acid and water. We do not discuss here the effect of polymer concentration on the UCST, but we will later report this effect for linear PEG.[11]

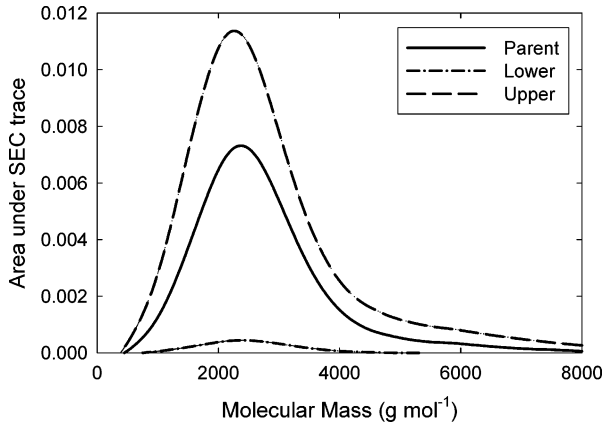

Figure 2. Four-arm star 2k PEG: area under SEC trace as a function of molecular mass for parent and daughter phases.

2. Fractionation of Star PEG in Isobutyric Acid and Water. Here we investigate the effects of chain branching on the partitioning and fractionation of PEG in isobutyric acid and water. Table 2 shows that equilibration times were reasonably short for all the samples: 1−2 days. The uncertainties in M_w and M_n are approximately 10%.

2.1. Four-Arm Star 2k PEG. At equilibrium (Figure 2), we observe the same trends for star PEG as seen previously for linear PEG at low average molecular mass.[10,11] Most of the polymer mass partitions into the upper isobutyric acid rich phase. There is no significant fractionation, the average molecular masses are the same in the daughter phases as in the parent phase, as is the case for linear PEG at this molecular mass.[11]

On the other hand, the partitioning is more pronounced for this star polymer than for the linear polymer of the same molecular mass. From the ratio of the areas under the molecular mass distribution (MMD) of each phase, the degree of partitioning for linear 2k PEG in isobutyric acid and water is $w_{lower} = 27 \pm 5\%$ and $w_{upper} = 73 \pm 5\%$ (errors given as one standard deviation), where w is the mass fraction of the total polymer in the sample.[11] Four-arm star 2k PEG partitions to a much greater extent: $w_{lower} = 2 \pm 1\%$ and $w_{upper} = 98 \pm 1\%$.

2.2. Six-Arm Star 4k PEG. When the number of arms is increased from four to six and the molecular mass is increased from 2 to 4 kg/mol, there is no significant change in behavior. The dramatic partitioning is still evident: $w_{lower} = 3 \pm 3\%$ and $w_{upper} = 97 \pm 3\%$. There is again no significant fractionation.

2.3. Six-Arm Star 10k PEG. The increase in the average molecular mass from 4 to 10 kg/mol has no effect on the partitioning: $w_{lower} \sim 1 \pm 1\%$ and $w_{upper} \sim 99 \pm 1\%$. No significant fractionation was observed, whereas for linear PEG at 10 kg/mol, we have observed a significant difference in M_w and M_n between the upper and lower phases.[11]

2.4. Four-Arm Star 10k PEG, Four-Arm Star 20k PEG, and Six-Arm Star 20k PEG. These samples all contained low molecular mass species that migrated into the upper isobutyric acid-rich phase and complicated the data analysis. The dramatic partitioning of star PEG does occur ($w_{lower} = 1.7 \pm 0.5\%$ and $w_{upper} = 98.3 \pm 0.5\%$ for four-arm star 10k PEG), but this includes the low molecular mass species. We do not list the partitioning and fractionation results for the 20k star PEG samples in Table 2, because the results were inconsistent due to the impurities present. However, there were indications of fractionation at 20 kg/mol average molecular mass.

2.5. Summary of Partitioning/Fractionation Studies. The star PEG samples showed partitioning between the two phases of isobutyric acid and water that is stronger than that of linear PEG samples of the same total molecular mass. The star PEG samples showed no significant fractionation at a molecular mass less than or equal to10 kg/mol, whereas linear PEG samples showed fractionation at molecular masses equal to or greater than 10 kg/mol.

The partitioning of linear PEG in isobutyric acid and water is related to the formation of helices in isobutyric acid.[12] The formation of helices in isobutyric acid is, in turn, related to formation of layers of hydration on the polymer molecules.[14] The increased partitioning for the star PEG can be due to the formation of more stable layers of hydration on the short arms of the star polymer than would form on the longer linear polymer molecules of the same overall molecular mass.

3. Small-Angle Neutron Scattering (SANS) of Star PEG in D_2O and in Deuterated Isobutyric Acid. Our previous SANS work showed that linear PEG forms coils in D_2O and stiff rods in deuterated isobutyric acid, and further analysis showed that these PEG rods are actually helices.[12,14] For linear PEG with average molecular masses of 20 kg/mol and greater in deuterated isobutyric acid, we observed the unfolding of the polymer helices into coils at temperatures between 55 and 60 °C. At a lower molecular mass of 2 kg/mol, the helices formed by linear PEG are stable to temperatures exceeding 60 °C. We now consider the SANS data for star PEG; the results are given in Tables 3 and 4.

3.1. Four-Arm Star 2k PEG. 3.1.1. Scaling Behavior of *I(q)* vs *q*. At 30 °C, the scattered intensity, $I(q)$, at intermediate q scales as $q^{-0.94}$ in deuterated isobutyric acid and as $q^{-1.70}$ in D_2O, indicating that the scattering species are coils in D_2O and rods in deuterated isobutyric acid. We interpret this to mean that the arms of the star PEG are coiled in D_2O and stiff in deuterated isobutyric acid. At high q, $I(q)$ scales as $q^{-4.21}$ in deuterated isobutyric acid and as $q^{-2.66}$ in D_2O; the former indicates the presence of a sharp interface between particle and solvent such as a stiff rod. On increasing the temperature to 60 °C, there is no change within experimental error (Table 3). The radius of gyration, R_g, as determined from Guinier analysis is twice as large in deuterated isobutyric acid as in D_2O, as we might expect for stiff helical arms as opposed to loosely coiled arms (Table 3).

From the scaling analysis, the arms of 4-arm star 2k PEG form coils in D_2O and rods (helices) in isobutyric acid. This is consistent with our expectations from prior work on linear PEG.[12,14]

3.1.2. Modeling. The SANS data for 4-arm star 2k PEG in D_2O are shown in Figure 3. Recall that the upturn at low q is due to aggregation, and thus those data are excluded from the fits.

The best fits of models for 4-arm star 2k PEG in D_2O at 30 °C are plotted in Figure 3 and listed in Table 4. The residual plots in Figure 3 show residuals that are almost all within 3 standard deviations, and thus the fits are good for all models. However, the residual plot for the model of Dozier et al. shows less systematic deviation than the other models. The Kratky plots in Figure 3d show even more convincingly that the Dozier et al. model best describes the data. As expected, there is a peak in $I(q)q^{5/3}$ for the star PEG in D_2O but not for a linear PEG sample in D_2O, as shown in Figure 3e. From the Dozier model, $\mu = 1/((\upsilon - 1) = -2.335 \pm 0.001$, so $\upsilon = 0.573 \pm 0.001$, which is in fair agreement with the theoretical value of $^3/_5$.[24]

The values of R_g^{arm} and R_g^{star} from the model fits to the data at 30 °C (Table 4) are the same within error as those determined from the Guinier analysis. Increasing the temperature to 60 °C

Table 3. Scaling of $I(q)$ vs q from SANS Data and Radius of Gyration, R_g (from a Guinier Plot) for Star PEG in D_2O and in Deuterated Isobutyric Acid (IBA-*d*) at Different Temperatures[a]

polymer	solvent	temperature	intermediate q scaling	high q scaling	R_g (Å) (Guinier)	expected species
4-arm star 2k	D_2O	30	-1.70 ± 0.06	-2.7 ± 0.4	18 ± 3	coils
		60	-1.68 ± 0.05	-3.4 ± 1.0	16 ± 3	coils
	IBA-*d*	30	-0.94 ± 0.02	-4.2 ± 0.3	32 ± 4	rods
		60	-0.92 ± 0.02	-4.6 ± 0.7	30 ± 5	rods
6-arm star 4k	D_2O	30	-1.6 ± 0.10	-2.0 ± 2.2	25 ± 6	coils
		60	-1.21 ± 0.07	-3.4 ± 0.7	26 ± 2	coils
	IBA-*d*	30	-1.18 ± 0.06	-5.0 ± 3.5	27 ± 13	rods
		60	-0.97 ± 0.07	-4.1 ± 0.7	33 ± 12	rods
4-arm star 10k[b]	D_2O	30	-1.91 ± 0.05	-2.7 ± 0.4	29 ± 3	coils
		60	-2.13 ± 0.04	-3.6 ± 0.5	30 ± 3	coils
	IBA-*d*	30	-1.02 ± 0.02	-4.3 ± 0.5	27 ± 5	rods
		60	-0.96 ± 0.02	-4.1 ± 0.4	36 ± 5	rods
6-arm star 10k	D_2O	30	-1.68 ± 0.03	-2.2 ± 0.6	38 ± 6	coils
		60	-1.75 ± 0.02	-3.1 ± 0.9	41 ± 5	coils
	IBA-*d*	30	-0.93 ± 0.01	-4.3 ± 0.6	43 ± 4	rods
		60	-1.02 ± 0.02	-4.0 ± 0.8	45 ± 5	rods

[a] Errors are quoted to 3 standard deviations (99% confidence). [b] Low molecular mass impurities present.

causes no change in the model fits or in the resulting parameters for 4-arm star 2 k PEG in D_2O.

There is no suitable model for star PEG in deuterated isobutyric acid, where the star arms are stiff; we rely on GIFT analyses (see below) in this case.

3.1.3. Inverse Fourier Transformation. The GIFT analysis for 4-arm star 2k PEG in D_2O is shown in Figure 4. The $p(r)$ closely resembles that of a sphere.[47−49,51] However, a sphere has a symmetric peak in $p(r)$, but there is asymmetry in this $p(r)$ and there is a second peak at larger values of r. The asymmetry could be caused by unequal arm lengths on the star polymer molecules. The second peak could be due to some aggregation of the star polymer molecules, showing up even though the low q data were not used in the analysis; this interpretation is supported by the decrease in the magnitude of this peak when the temperature is increased from 30 to 60 °C (Figure 4b), since we expect aggregation to decrease as temperature increases.

In D_2O, each arm of the star PEG forms a coil, and these four coils (connected at a central point) form an overall ellipsoidal scattering object. The maximum in $p(r)$ corresponds to the short axis radius of the ellipsoid, and the point at which $p(r)$ tends to zero gives the maximum particle dimension, D_{max}, or the long axis of the ellipsoid, as listed in Table 4.[47−49] The short axis remains unchanged between 30 and 60 °C, but the long axis decreases slightly, perhaps due to decreasing solvent quality. That the $p(r)$ profile does not yield a perfectly symmetrical form (and hence the star PEG does not form a spherical scattering particle) may be explained by differences in arm lengths; the models cannot detect this and yield averages for R_g^{arm} and R_g^{star}.

In deuterated isobutyric acid, we hypothesized that 4-arm star 2k PEG molecules will form stars with stiff arms, where the length of an arm is equal to the radius of gyration of the star polymer. The GIFT $p(r)$ profile for 4-arm star 2k PEG in deuterated isobutyric acid at 30 °C is shown in Figure 5, along with an illustration of the PEG conformation we envisage, stiff arms (rods) that are actually helices. The profile is unchanged at 60 °C. The $p(r)$ profile shows features that indicate a rigid rod, a sharp peak (related to the cross-section of the scattering rod) and a linear decrease with r (related to the rod axis).[47−49] We have previously observed this distinctive $p(r)$ for linear 2k PEG in deuterated isobutyric acid.[12,14] For a 4-arm star with tetrahedral geometry, the maximum particle dimension, D_{max}, where $p(r)$ tends to zero, is the distance between arms, ϵ. The length $L + h$ in Figure 5 is the total height of the tetrahedral, where L is the length of an arm, and accounts for the broad peak at about 62 Å. The point of inflection at about 14 Å corresponds to the cross-sectional diameter of an arm of the star, for which the radius is denoted R_{rod}.

The parameters from the GIFT analysis are: $R_{rod} = 7 \pm 2$ Å, L_{rod} (R_g^{star}) $= 50 \pm 2$ Å, and $\epsilon = 83 \pm 2$ Å. The errors are given to three standard deviations (99% confidence). The radius of gyration (or length of each rod) agrees with that determined from Guinier analysis ($R_g = 51 \pm 4$ Å). Assuming that the 4-arm star PEG forms a tetrahedral geometry, we calculate a value for ϵ by the cosine rule:

$$\epsilon = \sqrt{(a^2 + b^2 - 2ab\cos\theta)} \qquad (9)$$

where a and b are lengths of the rod (R_g^{star}) and θ is the angle between each arm (109°). Then the R_g^{star} obtained from this method gives $\epsilon = 82 \pm 5$ Å. This calculated value of ϵ is close to the observed value (GIFT analysis, D_{max}) of 82 ± 2 Å. The value of R_{rod} of 7 ± 2 Å is in good agreement with the radius (5.0 ± 0.9 Å, error given as 1 standard deviation) found for linear 2k PEG, folded into rods (helices) in deuterated isobutyric acid.[14]

3.2. Six-Arm Star 4k PEG. 3.2.1. Scaling Behavior of $I(q)$ vs q. The scaling of $I(q)$, given in Table 3, is consistent with flexible coils in D_2O and with rigid rods in deuterated isobutyric acid.

3.2.2. Modeling. Fits to all models are given in Table 4. In D_2O, the best fits to the Debye model for 6-arm star 4k PEG (Table 4) are consistent with the Guinier plots, and there is no noticeable temperature effect.

3.2.3. Inverse Fourier Transformation. In D_2O, the $p(r)$ profile for 6-arm star 4k PEG indicates ellipsoidal coils with dimensions larger than for the 4-arm 2k PEG (see Table 4).

In deuterated isobutyric acid at 30 °C, the $p(r)$ profile for 6-arm star 4k PEG (Figure 6) is similar to that for 4-arm star 2k PEG (Figure 5). However, at 60 °C, new features appear (Figure 6). Region A arises from the cross-section of a rigid rod: The point of inflection corresponds to the diameter of the rod.[48] Region B arises from the scattering of polymer coils, where the peak represents $R_g^{star}$of the PEG coils. This peak B becomes more intense as the temperature increases, consistent with our prior work, where we observed a rod-to-coil transition on heating for linear PEG.[12,14] The peak in region C represents the interarm spacing, ϵ. The point at which $p(r)$ goes to zero is

Table 4. Polymer Dimensions Determined from Five Methods of SANS Data Analysis[a,b]

			dimensions from models (R and D_{max} in Å; $I(0)$ in cm^{-1})				
polymer	solvent[c]	T (°C)	Guinier	Debye	Benoit	Dozier et al.	GIFT
4-arm 2k	D_2O	30	$R_g^{arm} = 18 \pm 3$ $R_g^{star} = 29 \pm 3$	$R_g^{arm} = 18.4 \pm 0.3$ $R_g^{star} = 29.1 \pm 0.3$ $I(0) = 0.094 \pm 0.002$ ($R^2 = 0.9872$)	$R_g^{arm} = 16.2 \pm 0.2$ $R_g^{star} = 25.6 \pm 0.2$ $I(0) = 0.088 \pm 0.001$ ($R^2 = 0.9915$)	$R_g^{arm} = 21.8 \pm 0.5$ $R_g^{star} = 34.5 \pm 0.5$ $\xi = 4.992 \pm 0.001$ $\mu = -2.335 \pm 0.001$ $\upsilon = 0.573 \pm 0.001$ $I(0) = 0.129 \pm 0.002$ ($R^2 = 0.9935$)	$R_{short} = 13 \pm 1$ $R_{long} = 34 \pm 1$
		60	$R_g^{arm} = 16 \pm 3$ $R_g^{star} = 25 \pm 3$	$R_g^{arm} = 18.7 \pm 0.4$ $R_g^{star} = 29.6 \pm 0.4$ $I(0) = 0.104 \pm 0.002$ ($R^2 = 0.9836$)	$R_g^{arm} = 16.4 \pm 0.1$ $R_g^{star} = 25.9 \pm 0.1$ $I(0) = 0.097 \pm 0.001$ ($R^2 = 0.9912$)	$R_g^{arm} = 21.8 \pm 0.5$ $R_g^{star} = 34.5 \pm 0.5$ $\xi = 4.992 \pm 0.001$ $\mu = -2.647 \pm 0.001$ $\upsilon = 0.6222 \pm 0.001$ $I(0) = 0.142 \pm 0.002$ ($R^2 = 0.9935$)	$R_{short} = 12 \pm 1$ $R_{long} = 30 \pm 1$
	IBA-*d*	30	$R_g^{arm} = 32 \pm 4$ $R_g^{star} = 51 \pm 4$	N/A	N/A	N/A	$R_{rod} = 7 \pm 2$ $R_g^{star} = 50 \pm 2$ $\epsilon = 83 \pm 2$ ($\epsilon_{calcd} = 82 \pm 5$)
		60	$R_g^{arm} = 30 \pm 5$ $R_g^{star} = 47 \pm 5$	N/A	N/A	N/A	$R_{rod} = 8 \pm 2$ $R_g^{star} = 45 \pm 2$ $\epsilon = 75 \pm 2$ ($\epsilon_{calcd} = 73 \pm 5$)
6-arm 4k	D_2O	30	$R_g^{arm} = 25 \pm 6$ $R_g^{star} = 41 \pm 6$	$R_g^{arm} = 22.3 \pm 0.6$ $R_g^{star} = 36.0 \pm 0.6$ $I(0) = 0.057 \pm 0.002$ ($R^2 = 0.9770$)	$R_g^{arm} = 19.1 \pm 0.4$ $R_g^{star} = 30.2 \pm 0.4$ $I(0) = 0.052 \pm 0.001$ ($R^2 = 0.9742$)	$R_g^{arm} = 24.3 \pm 0.9$ $R_g^{star} = 39.8 \pm 0.9$ $\xi = 5.00 \pm 0.02$ $\mu = -2.36 \pm 0.03$ $\upsilon = 0.58 \pm 0.001$ $I(0) = 0.074 \pm 0.002$ ($R^2 = 0.9802$)	$R_{short} = 13 \pm 3$ $R_{long} = 28 \pm 3$
		60	$R_g^{arm} = 26 \pm 2$ $R_g^{star} = 42 \pm 2$	$R_g^{arm} = 19.6 \pm 0.5$ $R_g^{star} = 31.0 \pm 0.5$ $I(0) = 0.151 \pm 0.004$ ($R^2 = 0.9790$)	$R_g^{arm} = 16.8 \pm 0.4$ $R_g^{star} = 27.6 \pm 0.4$ $I(0) = 0.138 \pm 0.004$ ($R^2 = 0.9664$)	$R_g^{arm} = 21.6 \pm 0.8$ $R_g^{star} = 34.1 \pm 0.8$ $\xi = 5.126 \pm 0.002$ $\mu = -2.69 \pm 0.01$ $\upsilon = 0.63 \pm 0.01$ $I(0) = 0.191 \pm 0.004$ ($R^2 = 0.9797$)	$R_{short} = 12 \pm 3$ $R_{long} = 26 \pm 3$
	IBA-*d*	30	$R_g^{arm} = 27 \pm 13$ $R_g^{star} = 44 \pm 13$	N/A	N/A	N/A	$R_{rod} = 7 \pm 2$ $R_g^{star,rod} = 40 \pm 2$ $\epsilon = 61 \pm 2$ ($\epsilon_{calcd} = 57 \pm 5$)
		60	$R_g^{arm} = 33 \pm 12$ $R_g^{star} = 54 \pm 13$	N/A	N/A	N/A	$R_{rod} = 7 \pm 2$ $R_g^{star,coil} = 27.0 \pm 2$ $R_g^{star,rod} = 42 \pm 2$ $\epsilon = 61 \pm 2$ ($\epsilon_{calcd} = 59 \pm 5$)
4-arm 10k[d]	D_2O	30	$R_g^{arm} = 29 \pm 3$ $R_g^{star} = 46 \pm 3$	$R_g^{arm} = 38.6 \pm 0.6$ $R_g^{star} = 61.0 \pm 0.3$ $I(0) = 0.457 \pm 0.001$ ($R^2 = 0.9966$)	$R_g^{arm} = 30.9 \pm 0.3$ $R_g^{star} = 48.9 \pm 0.3$ $I(0) = 0.374 \pm 0.005$ ($R^2 = 0.9977$)	N/A	$R_{short} = 33 \pm 2$ $D_{max} = 83 \pm 2$ $R_{long} = 42 \pm 2$
		60	$R_g^{arm} = 30 \pm 3$ $R_g^{star} = 47 \pm 3$	$R_g^{arm} = 39.9 \pm 0.8$ $R_g^{star} = 63.1 \pm 0.8$ $I(0) = 0.55 \pm 0.02$ ($R^2 = 0.9848$)	$R_g^{arm} = 31.5 \pm 0.4$ $R_g^{star} = 49.8 \pm 0.4$ $I(0) = 0.444 \pm 0.005$ ($R^2 = 0.9980$)	N/A	$R_{short} = 34 \pm 2$ $R_{long} = 42 \pm 2$
	IBA-*d*	30	$R_g^{arm} = 27 \pm 5$ $R_g^{star} = 43 \pm 5$	N/A	N/A	N/A	$R_{rod} = 7 \pm 2$ $R_g^{star,coil} = 25 \pm 2$ $R_g^{star,rod} = 75 \pm 2$ $\epsilon = 120 \pm 2$ ($\epsilon_{calcd} = 122 \pm 5$)
		60	$R_g^{arm} = 36 \pm 5$ $R_g^{star} = 57 \pm 5$	N/A	N/A	N/A	$R_{rod} = 7 \pm 2$ $R_g^{star,coil} = 25 \pm 2$ $R_g^{star,rod} = 68 \pm 2$ $\epsilon = 110 \pm 2$ ($\epsilon_{calcd} = 111 \pm 5$)

Table 4 (Continued)

			dimensions from models (R and D_{max} in Å; $I(0)$ in cm^{-1})				
polymer	solvent[c]	T (°C)	Guinier	Debye	Benoit	Dozier et al.	GIFT
6-arm 10k	D_2O	30	$R_g^{arm} = 38 \pm 6$	$R_g^{arm} = 42.1 \pm 0.8$	fit did not yield random residuals	fit did not yield random residuals	$R_{short} = 29 \pm 2$
			$R_g^{star} = 62 \pm 6$	$R_g^{star} = 68.8 \pm 0.8$ $I(0) = 0.426 \pm 0.006$ ($R^2 = 0.9958$)	fit did not yield random residuals	fit did not yield random residuals	$R_{long} = 50 \pm 2$
		60	$R_g^{arm} = 41 \pm 5$ $R_g^{star} = 67 \pm 5$	$R_g^{arm} = 43.8 \pm 0.5$ $I(0) = 0.507 \pm 0.008$ $R_g^{star} = 71.4 \pm 0.5$ ($R^2 = 0.9981$)			$R_{short} = 30 \pm 2$ $R_{long} = 55 \pm 2$
	IBA-*d*	30	$R_g^{arm} = 43 \pm 4$ $R_g^{star} = 70 \pm 4$	N/A	N/A	N/A	$R_{rod} = 7 \pm 3$ $R_g^{star,rod} = 83 \pm 3$ $\epsilon = 130 \pm 3$ ($\epsilon_{calcd} = 135 \pm 6$)
		60	$R_g^{arm} = 45 \pm 5$ $R_g^{star} = 73 \pm 5$	N/A	N/A	N/A	$R_{rod} = 7 \pm 3$ $R_g^{star,coil} = 27 \pm 3$ $R_g^{star,rod} = 87 \pm 3$ $\epsilon = 130 \pm 3$ ($\epsilon_{calcd} = 142 \pm 6$)

[a] The errors are given at 3 standard deviations. [b] See text for definitions of parameters and models. [c] IBA-*d* = deuterated isobutyric acid. [d] Low molecular mass impurities present.

the maximum particle dimension, D_{max}, which, from the geometry of a six-arm polymer, is equal to two times the rod length of the stiff star, $2R_g^{star}$. The dimensions obtained from the GIFT analysis are given in Table 4.

3.3. Four-Arm Star 10k PEG. Recall from above that this sample contained impurities of small molecular mass. We assume that these impurities were linear PEG molecules, which form coils in D_2O and helices in deuterated isobutyric acid.[12,14]

3.3.1. Scaling Behavior of *I(q)* vs *q*. The scaling of $I(q)$ is given in Table 3 and is consistent with flexible coils in D_2O and rigid rods in deuterated isobutyric acid.

3.3.2. Modeling. In D_2O, the fits to the Debye and Benoit models for 4-arm star 10k PEG are given in Table 4. The results are relatively consistent with the Guinier plots, and there is no noticeable temperature effect. The Dozier et al. model does not provide a reasonable fit, implying that the longer arms cannot be assumed to be uncorrelated.

3.3.3. Inverse Fourier Transformation. In D_2O, the $p(r)$ function is typical of an ellipsoid (see Table 4). In deuterated isobutyric acid, the $p(r)$ function indicates the coexistence of rods and coils at 30 °C and also at 60 °C, with the dimensions given in Table 4. Because of the coexistence of coiled and stiff arms on each star polymer, there are slight discrepancies between values of ϵ determined from the GIFT analysis and the values calculated from R_g^{star} from the GIFT analysis ($D_{max}/2$).

3.4. Six-Arm Star 10k PEG. 3.4.1. Scaling Behavior of *I(q)* vs *q*. The scaling of $I(q)$ is given in Table 3 and is consistent with flexible coils in D_2O and rigid rods in deuterated isobutyric acid.

3.4.2. Modeling. The best fits to the Debye model for 6-arm star 10k PEG in D_2O are given in Table 4 and are consistent with the Guinier plots. There is no noticeable temperature effect. The fits to the models of Benoit and Dozier et al. do not give random residuals and do not fit the data at all over the higher q regime. The Benoit model assumes no correlations among star arms, and the Dozier et al. model assumes a "blob" model for each arm, so both models may be less applicable when the number of arms increases from four to six and the total molecular mass (and thus the arm length) increases to 10 kg/mol.

3.4.3. Inverse Fourier Transformation. In D_2O, the $p(r)$ function is typical of an ellipsoid; see Table 4. In deuterated isobutyric acid at 30 °C, the $p(r)$ function indicates that only rods are present (Table 4). At 60 °C, a coexistence of rods and coils is again observed.

3.5. Summary of SANS Results. The SANS data support our hypothesis that the arms of the star PEG form coils in D_2O and form stiff rods (helices) in deuterated isobutyric acid. These arms are entirely rods for low molecular masses (2 kg/mol) and low temperatures (30 °C), but at higher molecular masses (4 kg/mol) and higher temperatures (60 °C), the rods revert partially to coils.

The SANS data for coiled arms can be modeled by the Debye, Benoit, and Dozier et al. models when there are four arms and the molecular mass is 2−4 kg/mol. When the molecular mass is 10 kg/mol and there are four arms, the Dozier et al. model no longer will describe the data. When the molecular mass is 10 kg/mol and there are six arms, neither the Benoit model or the Dozier model will describe the data. The failure of these models can be ascribed to increased correlations in the systems.

4. Polarimetry of Star PEG in H_2O and in Hydrogenated Isobutyric Acid. For all the star PEG samples in H_2O, there was no net optical rotation and hence no helical structure of the polymer.

4.1. Four-Arm Star 2k PEG in Isobutyric Acid. Figure 7 shows the net observed specific optical rotation, α, of polarized light as a function of temperature for 4-arm star 2k PEG in isobutyric acid doped with the chiral (*S*)-1,2-propanediol. The polarimetry data show that the PEG rotates the plane of polarized light and is thus chiral. The chirality of the PEG is taken to be due to the helicity of the star arms in isobutyric acid. The polarimetry data indicate that there is a decrease in helicity on heating but not a complete loss of helicity in this temperature range, which indicates a persistence of rods (helices) at these temperatures for this sample. Our previous work showed no helix−coil transition for linear PEG at molecular masses as low as 2 kg/mol.[12] The polarimetry results for 4-arm 2k star PEG (Figure 7) are also consistent with the SANS results for this

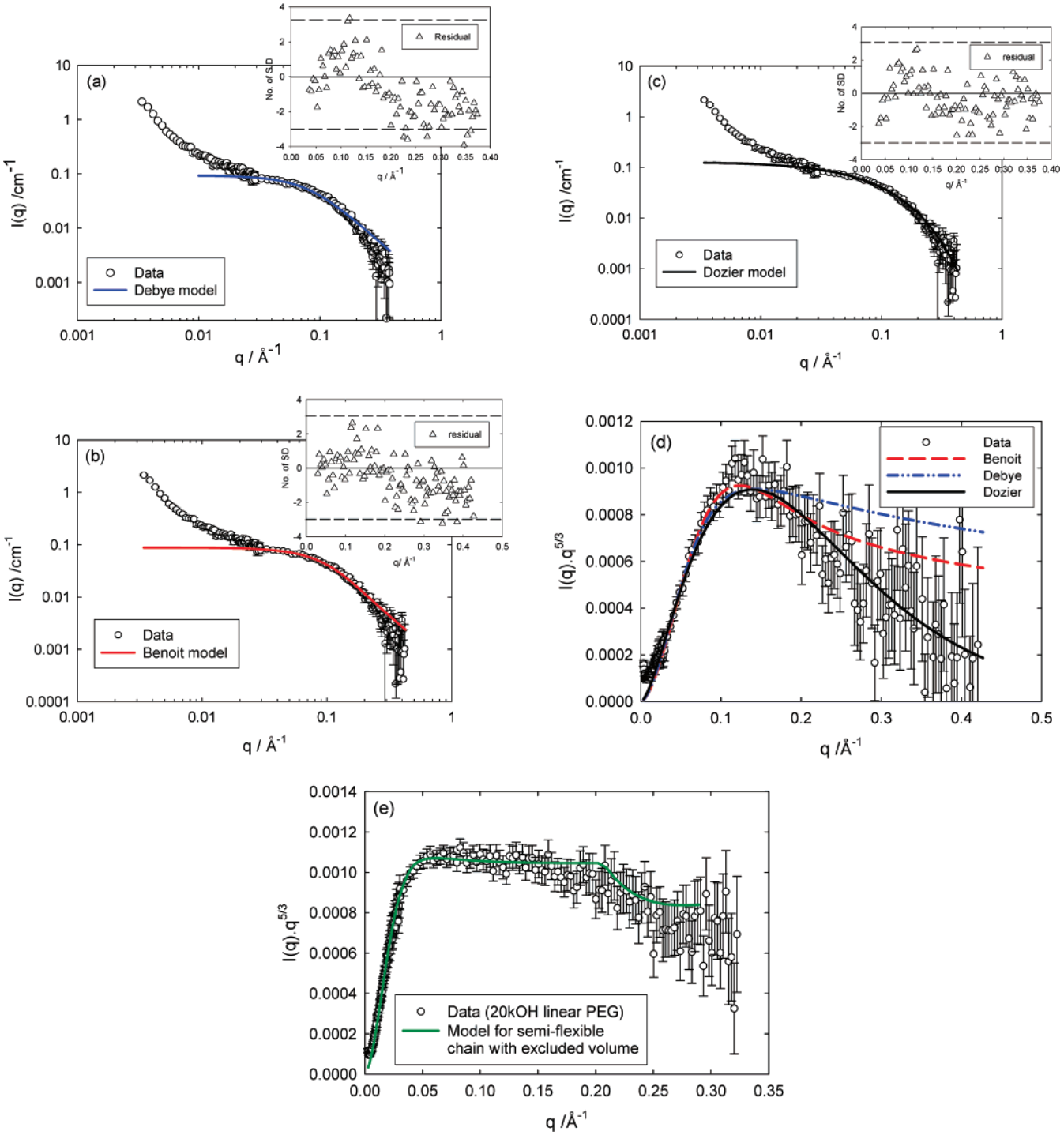

Figure 3. SANS profile for 4-arm star 2k PEG at 30 °C in D_2O. The ○ show the experimental data, and the solid lines (—) show the fits for (a) the Debye model for a polymer coil, (b) the Benoit model for a polymer star, (c) the Dozier et al. model for a polymer star, and (d) the Kratky plot with all corresponding models. (e) the Kratky plot for a linear polymer PEG in D_2O of $M_w = 23.8$ kg/mol and its corresponding fit to a semiflexible chain model[41] (sample 20k OH PEG in other papers[12,14]). The insets in parts a−c show the residual plots from the fits.

sample (Figure 5) in showing no uncoiling of the helical arms at these temperatures.

4.2. Six-Arm Star 4k PEG in Isobutyric Acid. Figure 8 shows that a conformational change does occur in 6-arm star 4k PEG in isobutyric acid at temperatures above about 65 °C. The net optical rotation approaches zero, indicating loss of helicity. This process is reversible and reproducible on a second heat−cool cycle. We interpret the disappearance of the optical rotation to an uncoiling of the helical star arms. These results are consistent with the SANS results (Figure 6) for this sample in showing that there is an uncoiling of the helical arms at higher temperatures but recall that the SANS experiment was done with deuterated isobutyric acid and the polarimetry was done with hydrogenated isobutyric acid.

4.3. Four-Arm Star 10k PEG in Isobutyric Acid. The specific optical rotation (data not shown) decreases with increasing temperature but does not go to zero. This indicates that the helicity of the star PEG decreases as a function of temperature but does not vanish over the temperature range 20−75 °C. This sample contained impurities of small molecular mass that probably were linear PEG molecules. Such low molecular mass PEG molecules could remain helical at these higher

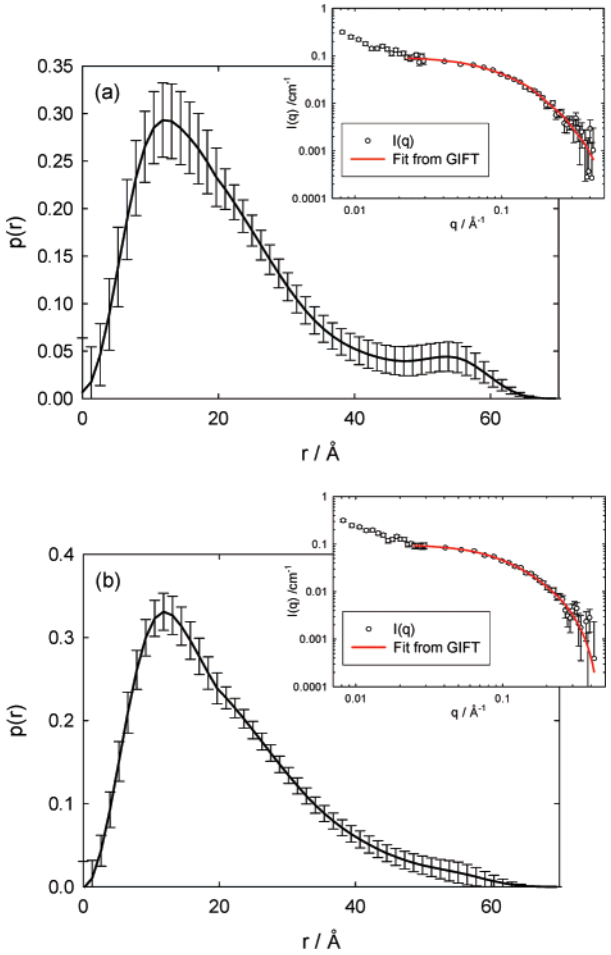

Figure 4. Pair distance distribution functions, $p(r)$, from GIFT for 4-arm star 2k PEG in D_2O at (a) 30 and (b) 60 °C. The insets are the fits to the data from the GIFT procedure. Only every third data point has been plotted for clarity.

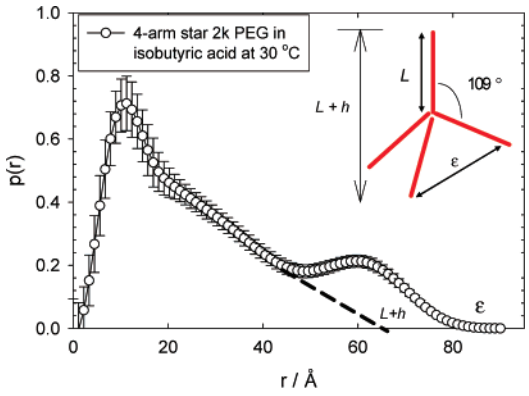

Figure 5. Pair distance distribution function, $p(r)$, from GIFT for 4-arm star 2k PEG in deuterated isobutyric acid at 30 °C. For clarity, only every third data point is shown. The inset shows the expected conformation of the star polymer in deuterated isobutyric acid.

temperatures.[12,14] The coexistence of coils and helices is consistent with the SANS results for this sample.

4.4. Six-Arm Star 10k PEG in Isobutyric Acid. The optical rotation (data not shown) decreases with increasing temperature and goes to zero at temperatures above about 70 °C. This is indicative of the helix-to-coil transition, and it is reproduced on a second heating−cooling cycle. This helix-to-coil transition is consistent with the SANS observation of coexisting rods and coils at 60 °C.

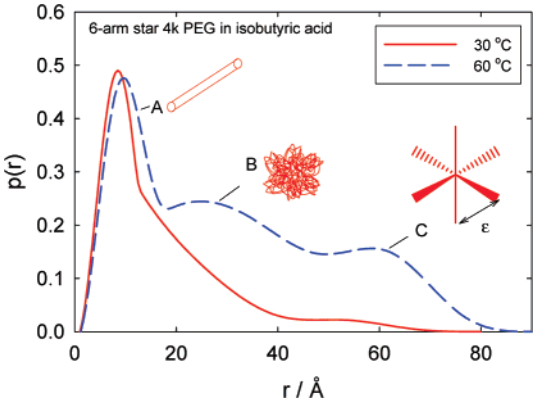

Figure 6. Pair distance distribution function, $p(r)$, for 6-arm star 4k PEG in isobutyric acid at 30 °C (solid red line) and 60 °C (dashed blue line).

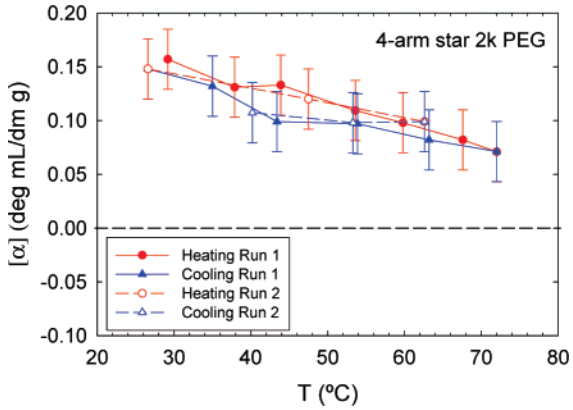

Figure 7. Polarimetry data for 4-arm star 2k PEG in isobutyric acid: the net optical rotation, α, as a function of temperature on heating and cooling runs.

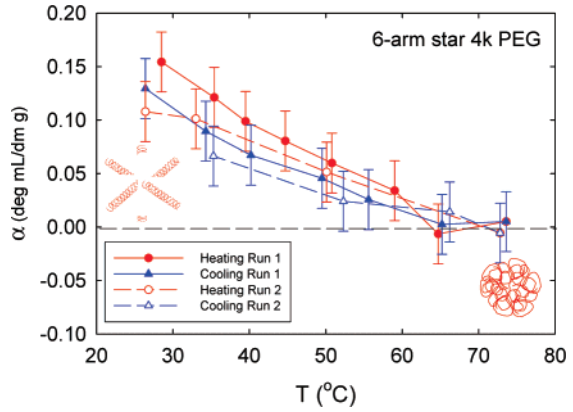

Figure 8. Polarimetry data for 6-arm star 4k PEG in isobutyric acid: the net optical rotation, α, as a function of temperature on heating and cooling runs. The insets to the figure show the PEG conformations at different temperatures.

4.5. Four-Arm Star 20k PEG and Six-Arm Star PEG in Isobutyric Acid. The helical structures (data not shown) are stable over the temperature range 20−75 °C. However, these samples also contained impurities that were probably low molecular mass linear PEG, which would remain helical at high temperatures.[12,14]

4.6. Summary of Polarimetry Studies. These experiments indicate that the arms of star PEG molecules form helices in isobutyric acid. These helical star arms are stable at higher temperatures than are the linear PEG helices of the same overall molecular mass. The chain length of each arm of the star polymer is shorter than the linear chain of the same molecular

mass (e.g., four-arm star PEG of molecular mass 2 kg/mol will have four arms, each arm being ~500 g/mol, whereas linear PEG of 2 kg/mol is one chain of 2 kg/mol). Since shorter PEG chains form more stable helices,[12,14] then the helical arms of star PEG are more stable than a linear helical chain of the same average molecular mass.

The 4-arm star PEG molecules form more stable helices than the 6-arm star molecules of the same total molecular mass. Linear PEG molecules are more stable at smaller molecular masses,[12,14] which would lead us to expect the 6-arm star PEG to form more stable helical arms than the 4-arm star PEG, since the molecular masses of the arms are smaller for the 6-arm star polymer. Perhaps the six helical arms are stabilized by their interactions.

Conclusions

We previously reported that for linear PEG, the large degree of partitioning and a dramatic fractionation are related to a conformational change of the polymer in the upper, isobutyric acid-rich phase.[11,12,14] Linear PEG has a coil conformation in water but has a helical conformation in certain solvents, including isobutyric acid, *n*-propanoic acid, and isopentanoic acid.[14] We have shown here that star PEG also partitions in two-phase mixtures of isobutyric acid and water and does so to a greater extent than does linear PEG of the same total molecular mass.[11,12] We did not observe fractionation of star PEG average molecular masses of 2−10 kg/mol, whereas we did observe fractionation of linear PEG at average molecular masses of 10 kg/mol and greater. We confirm that in water, the arms of star PEG molecules form coils, but that in isobutyric acid, the arms of star PEG form helices. At low molecular masses and low temperatures, all the arms form helices, but at higher molecular masses and temperatures, the arms are mixtures of coils and helices.

In D_2O, the star PEG coils have average molecular dimensions that do not change dramatically with either the temperature (30−60 °C) or the number of arms in the star polymer but that do increase with increasing molecular mass. In deuterated isobutyric acid, the radius of gyration for a "stiff" star polymer is larger than that of a coiled star polymer. The R_g^{star} of the stiff star PEG increases with increasing molecular mass but remains relatively unchanged as a function of temperature and number of arms in the polymer.

Star PEG molecules partition more than linear PEG molecules of the same molecular mass because the star arms are shorter polymer chains than linear PEG of the same molecular mass. PEG helices are stabilized by hydration layers of water, even trace water, in the solvent.[14] The shorter chains form more stable polymer helices because the shorter chains form more stable hydration layers.

Thus we have observed the first case of star polymers with stiff, helical arms. We have related these results to our earlier work on the folding of linear PEG into helical conformations.[12,14] We have only a qualitative understanding of how the hydration layers on the PEG molecules act to enable helical folding. We have no understanding of the details of this phenomenon, including why this happens only in particular solvents.[14]

Acknowledgment. This research was supported by the National Science Foundation, Chemistry Division. We also acknowledge support of the National Institute of Standards and Technology (NIST), U.S. Department of Commerce, in providing the neutron research facilities used in this work. Certain products and equipment are mentioned by name only to clarify the experimental conditions used; this does not mean that they are the best for the purpose or that NIST endorses them.

Supporting Information Available: Molecular weight (parent, lower, and upper phases) and *w* (parent, lower, and upper phases) values of PEG sample. This material is available free of charge via the Internet at http://pubs.acs.org.

References and Notes

(1) Mark, J. E.; Eisenberg, A.; Graessley, W. G.; Mandelkern, L.; Samulski, E. T.; Koening, J. L.; Wignall, G. D. *Physical Properties of Polymers*, 2nd ed.; American Chemical Society: Washington, DC, 1993.
(2) Mishra, M. K., Kobayashi, S., Eds. *Star and Hyperbranched Polymers*; Marcel Dekker: New York, 1999.
(3) Burchard, W. *Adv. Polym. Sci.* **1999**, *143*, 113−194.
(4) Grest, G. S.; Fetters, L. J.; Huang, J. S.; Richter, D. In *Advances in Chemical Physics: Polymeric Systems*; Prigogine, I., Rice, S. A., Eds.; John Wiley and Sons: New York, 1996; Vol. 44, pp 67−163.
(5) Sikorski, A.; Romiszowski, P. *J. Chem. Phys.* **1998**, *109*, 6169−6174.
(6) Ripoll, M.; Winkler, R. G.; Gompper, G. *Phys. Rev. Lett.* **2006**, *96*, 188302(1)−188302(4).
(7) Haws, J. R.; Wright, R. F. In *Handbook of Thermoplastic Elastomers*; Walker, B. M., Ed.; Reinhold: New York, 1979.
(8) Simms, J. A. *Prog. Org. Coatings* **1993**, *22*, 367−377.
(9) Merrill, E. W. *J. Biomater. Sci., Polym. Ed.* **1993**, *5*, 1−11.
(10) Shresth, R. S.; MacDonald, R. C.; Greer, S. C. *J. Chem. Phys.* **2002**, *117*, 9037−9049.
(11) Norman, A. I.; Manvilla, B. A.; Frank, E. L.; Niamke, J. N.; Smith, G. D.; Greer, S. C. *Macromolecules*, accepted for publication.
(12) Alessi, M. L.; Norman, A. I.; Knowlton, S. E.; Ho, D. L.; Greer, S. C. *Macromolecules* **2005**, *38*, 9333−9340.
(13) Castellanos, P.; Norman, A. I.; Greer, S. C. *J. Phys. Chem. B* **2006**, *110*, 22172−22177.
(14) Norman, A. I.; Fei, Y.; Ho, D. L.; Greer, S. C. *Macromolecules* **2007**, *40*, 2559−2567.
(15) Jacobs, D. T. *J. Chem. Phys.* **1989**, *91*, 560−563.
(16) Venkatesu, P. *J. Chem. Phys.* **2005**, *123*, 024902(1) − 024902(10).
(17) Venkatesu, P. *J. Phys. Chem. B* **2006**, *110*, 17339−17346.
(18) Dobashi, T.; Nakata, M.; Kaneko, M. *J. Chem. Phys.* **1984**, *80*, 948−953.
(19) To, K.; Choi, H. J. *Phys. Rev. Lett.* **1998**, *80*, 536−539.
(20) To, K. *Phys. Rev. E* **2001**, *63*, 026108(1)−026108(4)
(21) Staikos, G.; Skondras, P.; Dondos, A. *Makromol. Chem.* **1982**, *183*, 603−609.
(22) Dondos, A.; Izumi, Y. *Makromol. Chem.* **1980**, *181*, 701−706.
(23) Izumi, Y.; Dondos, A.; Picot, C.; Benoit, H. *Makromol. Chem.* **1979**, *180*, 2483−2490.
(24) Flory, P. J. *Principles of Polymer Chemistry*; Cornell University Press: Ithaca, NY, 1953.
(25) Case, L. C. *J. Phys. Chem. B* **1958**, *62*, 895−896.
(26) Case, L. C. *Makromol. Chem.* **1960**, *41*, 61−76.
(27) Rintzler-Yen, D.; Raghavan, S.; Merrill, E. W. *Macromolecules* **1996**, *29*, 8977−8978.
(28) Cansell, F.; Botella, P.; Six, J.-L.; Garrabos, Y.; Tufeu, R.; Gnanou, Y. *Polym. J.* **1997**, *27*, 910−913.
(29) Daneshvar, M.; Gulari, E. *J. Supercrit. Fluids* **1992**, *5*, 143−150.
(30) Venkataraman, T. S.; Narducci, L. M. *J. Phys. C: Solid State Phys.* **1977**, *10*, 2849−2861.
(31) Greer, S. C. In *Building Scientific Apparatus: A Practical Guide to Design and Construction*, 3rd ed.; Moore, J. H., Davis, C. C., Coplan, M. A., Eds.; Perseus Books: Cambridge, MA, 2002; pp 581−606.
(32) Norman, A. I.; Ho, D. L.; Karim, A.; Amis, E. J. *J. Colloid Interface Sci.* **2005**, *288*, 155−165.
(33) Guinier, A.; Fournet, G. *Small-Angle Scattering of X-rays*; John Wiley and Sons: New York, 1955.
(34) Beaucage, G. *J. Appl. Crystallogr.* **1995**, *28*, 717−728.
(35) Porod, G. *Kolloid-Z.* **1951**, *124*, 83−114.
(36) Higgins, J. S.; Benoit, H. C. *Polymers and Neutron Scattering*; Clarendon Press: Oxford, U.K., 1994.
(37) Dozier, W. D.; Huang, J. S.; Fetters, L. J. *Macromolecules* **1991**, *24*, 2810−2814.
(38) Richter, D.; Stuhm, B.; Ewen, B.; Nerger, D. *Phys. Rev. Lett.* **1987**, *58*, 2462−2465.
(39) Willner, L.; Jucknischke, O.; Richter, D.; Roovers, J.; Zhou, L. L.; Toporowski, P. M.; Fetters, L. J.; Huang, J. S.; Lin, M. Y.; Hadjichristidis, N. *Macromolecules* **1994**, *27*, 3821−3829.

(40) Rathgeber, S.; Monkenbusch, M.; Kreitschmann, M.; Urban, V.; Brulet, A. *J. Chem. Phys.* **2002**, *117*, 4047−4062.
(41) Pedersen, J. S.; Schurtenberger, P. *Macromolecules* **1996**, *29*, 7602−7612.
(42) Roe, R.-J. *Methods of X-ray and Neutron Scattering in Polymer Science*; Oxford University Press: New York, 2000.
(43) Benoit, H. *J. Polym. Sci.* **1953**, *6*, 507−510.
(44) Daoud, M.; Cotton, J. P. *J. Phys.* **1982**, *43*, 531−538.
(45) Hammouda, B.; Ho, D.; Kline, S. *Macromolecules* **2002**, *35*, 8578−8585.
(46) Ho, D. L.; Hammouda, B.; Kline, S. R. *J. Polym. Sci., Part B: Polym. Phys.* **2003**, *41*, 135−138.
(47) GIFT software available from O. Glatter, University of Graz, Austria. Details can be found at the website http://physchem.kfunigraz.ac.at/sm/.
(48) Glatter, O. In *Neutrons, X-rays, and Light: Scattering Methods Applied to Soft Condensed Matter*; Lindner, P., Zemb, T., Eds.; Elsevier: Amsterdam, The Netherlands, 2002; pp 103−124.
(49) Weyerich, B.; Brunner-Popela, J.; Glatter, O. *J. Appl. Cryst.* **1999**, *32*, 197−209.
(50) Balasubramanian, D.; Mitra, P. *J. Phys. Chem. B* **1979**, *83*, 2724−2727.
(51) Hansen, S. *J. Appl. Crystallogr.* **2003**, *36*, 1190−1196.

MA071568W